RESEARCH ARTICLE OPEN ACCESS

Dynamic MR Visualization and Detection of Upper Airway Obstruction during Sleep Using Region-Growing Segmentation

[1] B. Jefferson, [2]K. Appasamy, [3]A. Bathsheba Parimala,
Assistant professor , Department of BCA & M.SC(NT&IT), St . Johns College ,Palayamkottai.

Abstract:

Obstructive Sleep Apnea(OSA) syndrome is a common breathing disorder in which the airflow pauses during sleep due to physical collapse of pharyngeal airway. Recently, dynamic MRI of the upper airway has been demonstrated during natural sleep, with sufficient fourth dimensional resolution not tending to spread the study patterns of airway obstruction in adults with OSA. In this project, we use open source multi-seeded region growing segmentation approach, where the operator selects a region of interest that includes the pharyngeal airway, by placing three seeds in the patent airway, and determines a threshold for the first frame in order to determine the collapsed tissues which blocks the airway path. This simple automated segmentation technique enhances the process of dynamic MRI studies of the pharyngeal airway and enables diagonising of obstructive events with the collapse plot. Region growing results well in Cosine Coefficients compared with manual segmentation of 1. It automatically detect 90% of collapse events. This approach leads to segment the airway path efficiently. It uses long MRI scans in order to diagnosis the collapsed events with brief, accurate details in a short span of time.

Keywords **— Obstructive sleep apnea, Cosine coefficients, Open source multi-seeded implementation, MRI- Magnetic Resonance Imaging.**

I. INTRODUCTION

Obstructive sleep apnea (OSA) (or apnea) is the most common type of sleep apnea and is caused by complete or partial obstructions of the upper airway. It is characterized by repetitive episodes of shallow or paused breathing during sleep, despite the effort to breathe, and is usually associated with a reduction in blood oxygen saturation. These decreased breathing called "apneas" (literally, "without breath"), typically last 20 to 40 seconds. It is often recognized as a problem by others who see the individual during episodes or is suspected because of its effects on the body. OSA is commonly accompanied with snoring. OSA is associated with symptoms during the daytime. It affects approximately 4–9% of adults [2] and 2% of children [3] in the United States; in particular, OSA has been reported in 13–66% of obese children [4]. OSA is linked to decreased productivity, accidents, and increased risk of cardiovascular disease . It is widely recognized that determining the accurate location of obstruction sites may benefit treatment planning and patient outcome . The current gold standard for diagnosing OSA is overnight polysomnography (PSG). PSG involves monitoring and continuously recording several physiological signals that reflect sleep and breathing, for roughly 7–8 h. The single most important output of overnight PSG is the apnea-hypopnea index (AHI)— the average number of complete or partial obstructive events that occur per hour during sleep. PSG also helps to elucidate the impact of these events on sleep pattern and gas exchange. An overnight PSG requires interpretation by a skilled sleep specialist for visual scoring; in contrast, computer scoring has not been proven accurate. Three dimensional static CT images of the UA were segmented for volumetric analysis using level-set-based deformable models [17]. In [3] and [20], static 3-D T2-weighted MR images were segmented using a fuzzy connectedness-based algorithm that required 4 min/study. This framework required significant operator and processing time, even for short scans. Wagshul *et al.* used threshold-based segmentation to segment and depict 3-DUAimages of tidal breathing [11]. Their static 3-D and retrospectively gated UA images had significantly higher contrast-to-noise ratio (CNR) and reduced artifacts compared to what is seen in real-

time 3-D UA MRI. Additionally, these previous methods were not designed for or applied to collapsed airways. In this study, we demonstrate visualization of UA dynamics and detection of natural obstructive apneas during sleep. The key development is a method for semiautomated analysis of realtime UA MRI using multi-seeded region growing. Region growing was chosen for its simplicity to demonstrate a new application where segmentation facilitates the workflow of a novel study. Multiple seeds were found to enable more accurate segmentation and visualization during collapse events when the airway is divided into two (or more) patent sections. We narrow the analysis volume to just the pharyngeal airway and propagate seeds from one time frame to the next using the observation that the nasal cavity and base of the airway remain patent at all times. We demonstrate that this approach performs as well as manual segmentation. Errors were comparable to intraoperator variability of manual segmentation. We also show that it enables analysis of long scans and visualization of important factors in an MRI sleep study, such as the time, site, and extent of airway collapse.

The rest of the paper is organized as follows. Section II discusses the related work. Section III discusses about proposed region growing segmentation and selection of seed points. Section IV discusses the simulation results for the detection of obstruction in the pharyngeal tract as collapse plot. Conclusions are drawn in the last section.

II. RELATED WORKS

S. Y. Yeoa et al.[17], proposed that Segmentation of human upper airway using a level set based deformable model uses a hypothesized dynamic interaction force between the deformable surface and object boundaries which can greatly improve the deformable model performance in acquiring complex geometries, boundary concavities, and in dealing with weak image edges. It has an efficient segment complex and compact structures, easily deal with weak image edges and reduces the computational expenses. It requires processing time, even for short scans. Y.-C. Kim et al.[13], proposed that an MR imaging protocol is presented that simultaneously acquires dynamic airway images and relevant physiological signals and it is compatible with an external airway occlusion setup. It is susceptible to imperfect placement of the imaging slices. It has larger dynamic range of samples. It has better image quality. It suffer from gaps in coverage. Sonia Maria G.P. Togeiro, Cauby M. et al., proposed that evaluation of the upper airway in obstructive sleep apnea provide information about anatomic abnormalities and the level of pharyngeal narrowing or collapse while the patient is awake or asleep. It has an adequate image quality for segmenting the upper airway. It has high complexity. Y.-C. Kim et al.[15], proposed real-time 3D magnetic resonance imaging (MRI) with simultaneous recording of physiological signals for identifying sites of airway obstruction during natural sleep in pediatric patients with sleep-disordered breathing. It perform average volume reductions. Y.-C. Kim et al.[14], proposed that Obstructive sleep apnea (OSA) is a disease in which the upper airway (UA) narrowing/collapse induces reduction/cessation of air flow and an increased ventilatory drive leading to frequent arousals during sleep. Computational time is more. R. Arens et al.[3], proposed that Magnetic resonance imaging and automatic segmentation is used to define the upper airway.The upper airway has a complex shape formed by various tissues with heterogeneous compositions that surround the air column. It depicts about static images of tidal breathing. R. J. Schwab et al.[7] proposed A sophisticated volumetric analysis technique with magnetic resonance imaging is utilized. MR imaging and computer based analysis techniques allowed to objectively quantify the volume of the tongue, soft palate, Para-pharyngeal, fat pads and lateral pharyngeal walls. It involves analysis using volumetric magnetic resonance imaging. Y.-C. Kim et al[14].,proposed Sleep-related breathing disorders (SRBD) in children have five phenotypes: primary snoring, hypoventilation, high arousal frequency, obstructive sleep apnea, and central sleep apnea. It does not provide direct information of the upper airway anatomy. Overnight polysomnography is widely used to determine SRBD phenotype and its severity.

III. PROPOSED REGION GROWING SEGMENTATION

A region of interest (ROI) is selected from the hard palate to the epiglottis in the mid-sagittal slice of the reference frame. Two seeds are placed within the mid-sagittal slice: one in the nasopharyngeal airway and the other in the oropharyngeal airway. The first frame is segmented using multi-seeded 3-D region growing. The threshold is manually set to separate air and tissue signals in the ROI. The two initial seeds plus the two new seeds are used for segmentation. This process repeats until all frames are processed. Segmentation is performed using an open-source implementation multiseeded 3D region growing .

Open source multi-seeded implementation is a simple region-based image segmentation method. It is also classified as a pixel-based image segmentation method since it involves the selection of initial seed points. It is the technique used to segment airway

path and collapsed events by placing 3 seeds in the pharyngeal tract. Threshold value is used to turn a gray-scale image into a binary image inorder to separate airway path and collapsed tissues. This approach to segmentation examines neighboring pixels of initial seed points and determines whether the pixel neighbors should be added to the region. The main aim of the segmentation approach is to segment an image into regions. The segmentation method looks for the boundaries between regions based on discontinuities in grayscale or color properties to partition the obstruction in the pharyngeal tract. Region-based segmentation is a technique for determining the region directly. The basic formulation is:

(a) $\bigcup_{i=1}^{n} R_i = R$
(b) R_i is a connected region, i=1,2,….n

(c) $R_i \cap R_j = \emptyset$ for all i=1,2,… n
(d) $P(R_i)$ = TRUE for i = 1,2,..n
(e) $P(R_i \cup R_j)$ = FALSE for any adjacent region R_i and R_j.
(f) $P(R_i)$ is a logical predicate defined over the points in set R_i and $\emptyset$ is the null set.

a) Means that the segmentation must be complete; that is, every pixel must be in a region.
b) It requires that every points in a region which must be connected in some predefined criteria.
c) The regions should be disjoint.
d) Deals with the properties that must be satisfied by the pixels in a segmented region. For example $P(R_i)$ = TRUE if all pixels in R_i have the same grayscale.
e) Region R_i and R_i are different with the predefined sense of predicate P.

SELECTION OF SEED POINTS:

The first step involves in the region growing is to select a set of seed points. Seed points selection is based on some user criterion pixels in a certain grayscale range, pixels evenly spaced on a grid. The initial region starts from the exact location of these placed seed points and it grows from these seed points to adjacent points followed by region membership criterion. It includes the region of interest comprises of the oropharyngeal path, the mid-sagittal slice and the nasopharyngeal path . Here we use 4-connected neighborhood to grow from the seed points. We may also opt 8-connected neighborhood for the pixels adjacent relationship. The criteria considers the same pixel value within the regions .The adjacent pixels of seed points is continuously reviewing by the user. If the adjacent pixels also have the same intensity value with the seed points, we considers them and classifies it into the seed points. It is an iterated process until there are no change in two successive iterative stages. Eventhough the criteria varies inaccordance with the approach, the main aim is to classify the similarity of the image into regions.

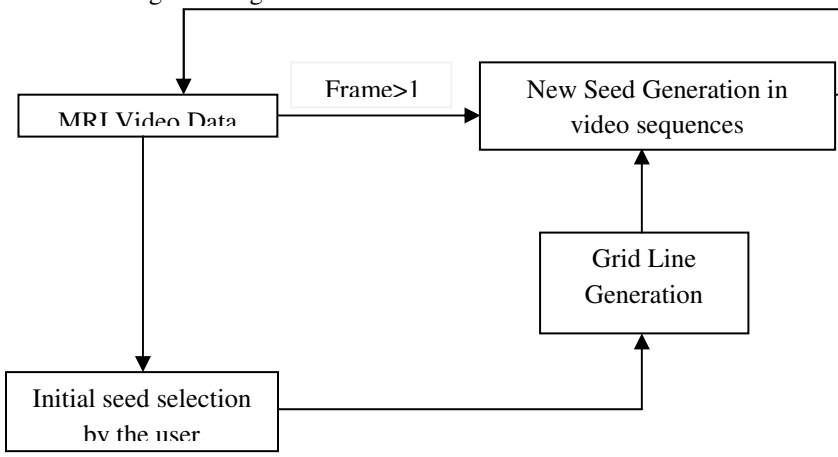

Fig 1. FLOW DIAGRAM OF SEGMENTATION

In this proposed system, Image is acquired as frame from the MRI video data. From that frames the 1st frame is captured for Initial seed Selection which will be performed by the User and then the Grid lines are generated from the 1st frame, Region of Interest (ROI) is selected from the hard palate to the epiglottis in the mid-sagittal slice,then the new seed will be generated in the video sequences from the generated grid lines. First frame is segmented using multiseeded 3D region growing.

Three seeds are selected in the pharyngeal tract: one in the nasopharyngeal airway, one in the oropharyngeal airway and another in the mid-sagittal slice.Except the first frame, all the next frames are given for new seed generation of video sequences in the block. Threshold is manually set to separate air and tissues signals in the ROI, between 7th and 15th percentiles of pixel intensities. Seeds are generated automatically, by dividing segmented airway into 5 sections and placing 2 new seeds at the centroid with largest volume. Two initial and two new seeds are taken for segmentation.From the constructed grid line airway path is detected.oropharyngeal(lip) and nasopharyngeal(larynx) are traced and tracked in order to detect the obstructive events which blocks the airway. Collapse plot specifies the Obstructive events in the grid lines between the oropharyngeal airway path and nasopharyngeal airway path.We proposed a data set of 240 frames with 2mins of data where selected to demonstrate and a long scan of

10mins/frame to obtain the accurate sleep state disorder changes .

COSINE COEFFICIENTS

Cosine coefficients is a measure of similarity between two non-zero vectors of an inner product space that measures the cosine of the angle between them. It is used to compare this automated segmentation with manual segmentation. For two segmented volumes A and B, the cosine coefficients is given by $\frac{|X \cap Y|}{|X|^{1/2}\,|Y|^{1/2}}$ and quantifies the amount of overlap between the two sets. The CC ranges from 0 to 1, where 1 signifies exact overlap between A and B, and 0 signifies no overlap. A CC of 0.60 or greater is considered to be "very good." in Cosine Coefficients of 0.65 to 0.72 It automatically detect 90% of collapse events. Sensitivity of the method to seed selection was also evaluated using ten different pairs of seed point.

IV. RESULTS AND DISCUSSIONS

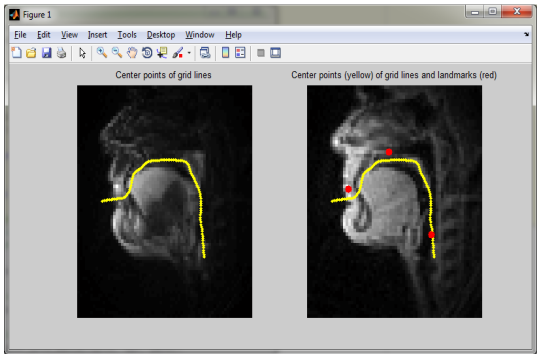

Fig:2 Center points of grid lines Fig:2(a)Center points of grid lines and landmarks

Fig:2 illustrates that constructing the centre points of grid lines using the region of interest in a semi automated manner by the user with appropriate intensity of pixels in black and grey scale image of the pharyngeal tract. For single plane image, 0-80 pixels - black image ; 80-180 pixels - grey image ; 180-255 pixels - white image .

Fig:2(a)illustrates that by placing seed points in the tract, one in the hard palatte, one in the soft palatte, another in the mid -sagittal slice since it is a open source implementation of multiseeded 3D region growing.

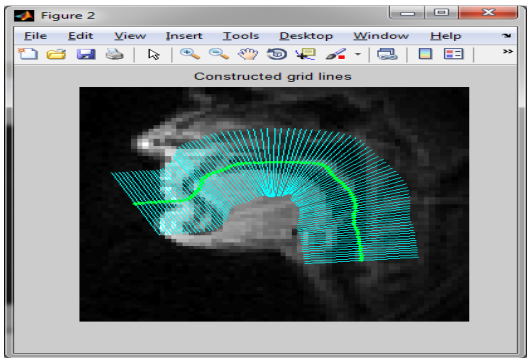

Fig:3 Constructed grid lines

Fig:3 illustrates that input AVI data is sent as matrix file consists of image frames as an input data. At a time, it reads only a single frame. The path is set for input directory and output directory separately. N dimensional DCT smoothing is done in the airway path. It defines the centre of bin point co ordinate of gridline. It plots intensity of each gridline depends on pixels. Moving average filter is used for smoothing the constructed grid lines. It assigns simpler variable names, adds extra points for each sides, determines inner and outer boundaries for each bin point co ordinate of grid line

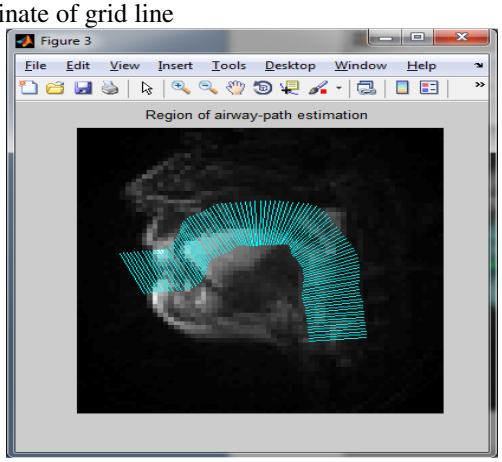

Fig:4 Region of airway-path estimation

Fig:4 illustrates that the estimation of airway path which includes oropharyngeal airway and nasopharyngeal airway. Smoothing is performed to Smoothing is done using x-frames, y-grids, z-bits. Smoothing of Object Likelihood algorithm reshapes the airway path. Viterbi decoding starts at this path and this is used to detect the best state path.

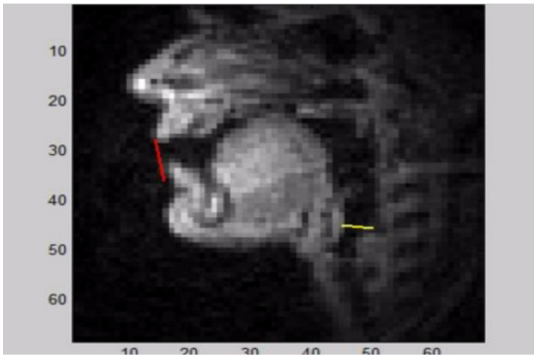

Fig:5 Lip-pharynx Initialization

Fig:5 illustrates illustrates that the initialize the path of lip and larynx(respiratory path). Lip and Larynx will have different path for detecting the obstructive events.From the constructed grid line initialization of lip and larynx will starts by setting the threshold by 2mm above and below.Transition matrix is computed to determine the Eucledian distance between adjacent pixels.In each grid line,maximum intensity in the search region is computed.Apart from the above steps,sigmoid fuction of the transistion matrix is done in larynx initialization.

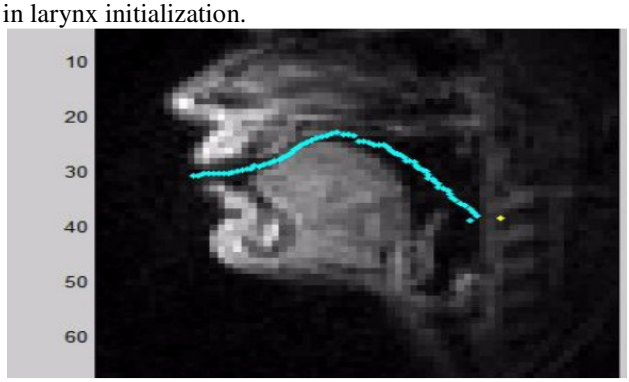

Fig:6 Airway Path Detection

Fig:6 illustrates the detection airway path using threshold in order to separate air and tissue signals in the ROI. It includes PCA based noise reduction, pixel sensitivity correction which involves M by N neighborhood around the corresponding pixels. Sigmoid Warping function parameters for transition past of airway path estimation in the region from the alveolar ridge landmark point to the front most edge of the lips.

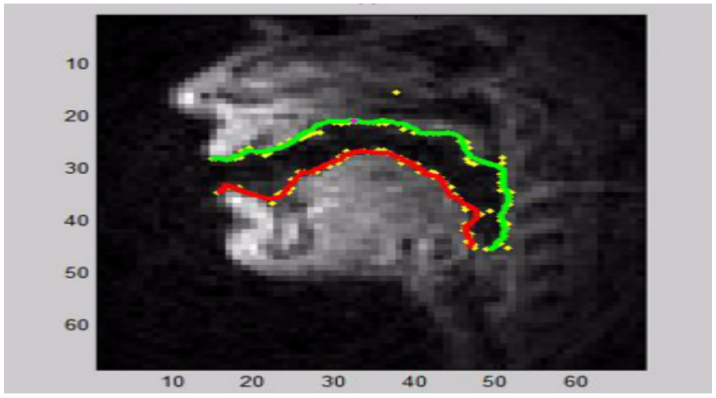

Fig:7 Airway Segmentation

Fig:7 illustrates the segmentation of airway path with high signal intensity to detect the obstructive events of the pharyngeal tract. Tissue airway boundary estimation involves threshold of 0.5 where the boundary is determined, Span X pixels from the center to its each side is 6.DCT smoothing involves maximum number of clusters of frames for pharyngeal wall boundary.

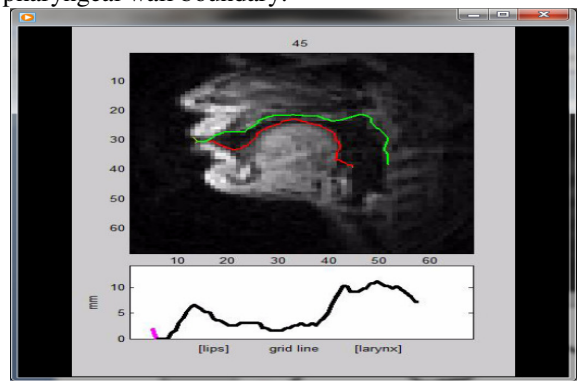

Fig:8 Segmentation with Collapse Plot

Fig:8 illustrates that the binary collapse plot to navigate collapse events and visualize the precise site and extent of collapse. Reconstruct image using weighted components. Minimum Euclidian distance for this segmentation is set at 1000.

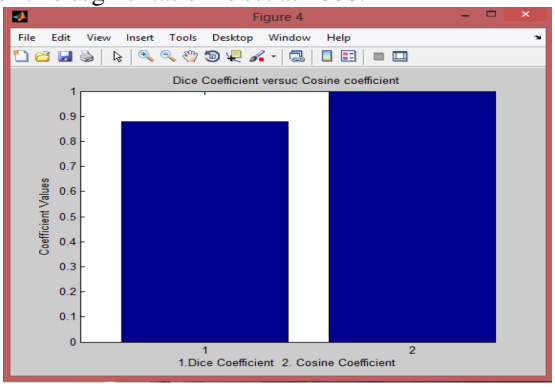

Fig. 9 Dice coefficient versus Cosine coefficient

Fig. 9 illustrates the difference between the Dice and Cosine Coefficient. In the existing system they use

Dice coefficient method and they obtained 0.9 which means that detects 90% of collapse plot. But in our proposed system, this makes use of Cosine Co-efficient method and this obtained a value 1 which means this detects 100% of collapse plot. Thus the proposed method has shown very good increment from the existing system with manual segmentation.

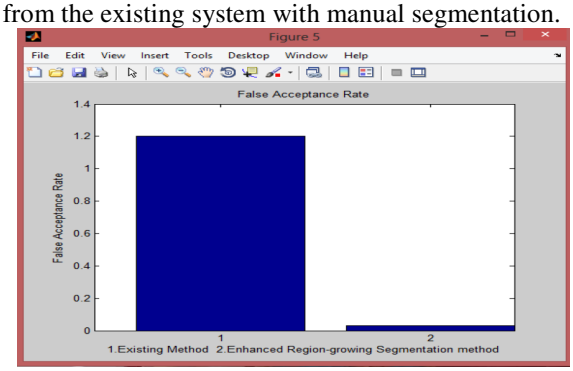

Fig.10 False acceptance rate

Fig.10 illustrates the False acceptance Rate of the Existing system and the Enhanced Region-Growing Segmentation method. False acceptance rate is the segmentation error occurred during the process. The false acceptance rate of the Existing Method and the Enhanced Region-growing Segmentation method is in the ratio of 1.2:0.1 which clearly describes that the false acceptance rate for the proposed system is variably lesser than the Existing system.

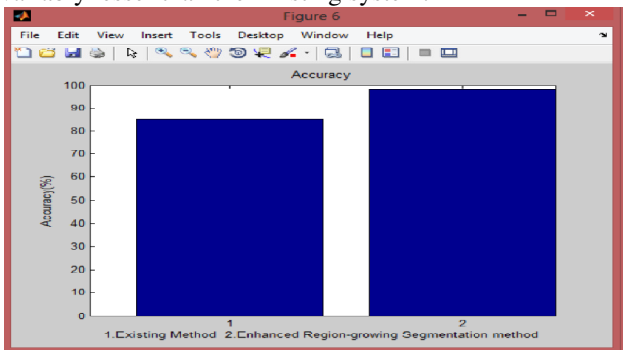

Fig.11 Accuracy of segmentation

Fig.11 illustrates the percentage of accuracy between the Existing Method and the Enhanced Region-growing Segmentation Method. The accuracy depends on the diagnosis of the collpase plot. The accuracy of the Existing system is 85% with is good but in the Proposed system we make the accuracy better in order to get the overall obstruction and the percentage of the accuracy of the Enhanced Region-growing Segmentation Method is 98%.Thus the accuracy is comparably high.

V. CONCLUSION

We have demonstrated a novel and simple automated segmentation approach for dynamic MRI of the pharyngeal airway. The proposed method has shown very good agreement with manual segmentation. This approach for the first time, enables time-efficient identification of collapse events and enables visualization of the pharyngeal airway dynamics throughout all events. The binary collapse plot makes it easier to navigate to collapse events and the visualizations allow us to observe the precise site and extent of collapse. Detection based on the existence of four connected regions that were larger than 0.2cm^3. When airway is patent, region growing results in a single contiguous region. Region growing methods can correctly separate the regions that have the same properties we define. Region growing methods can provide the original images which have clear edges with good segmentation results. The concept is simple. We only need a small number of seed points to represent the property we want, then grow the region. We can determine the seed points and the criteria we want to make. We can choose the multiple criteria at the same time. The segmented dynamic MR data can provide previously unavailable anatomical landmarks for clinical interventions such as surgery or oral appliances in the treatment of OSA or for patient-specific modeling of the airway collapse pattern.

REFERENCES:

[1] A. Malhotra and D. P. White, “Obstructive sleep apnoea,” Lancet, vol. 360, no. 9328, pp. 237–245, Jul. 2002.

[2] R.Arens and C. L.Marcus, “Pathophysiology of upper airway obstruction: A developmental perspective,” Sleep, vol. 27, no. 5, pp. 997–1019, Aug. 2004.

[3] R. Arens et al., “Upper airway size analysis by magnetic resonance imaging of children with obstructive sleep apnea syndrome,” Am. J. Respir. Crit. Care Med., vol. 167, no. 1, pp. 65–70, Jan. 2003.

[4] S. L. Verhulst et al., “Sleep-disordered breathing in overweight and obese children and adolescents: Prevalence, characteristics and the role of fat distribution,” Arch. Dis. Child., vol. 92, no. 3, pp. 205–208, Mar. 2007.

[5] T. D. Bradley and J. S. Floras, “Obstructive sleep apnoea and its cardiovascular consequences,” Lancet, vol. 373, no. 9657, pp. 82–93, Jan. 2009.

[6] A. N. Rama et al., “Sites of obstruction in obstructive sleep apnea,” Chest, vol. 122, no. 4, pp. 1139–1147, Oct. 2002.

[7] R. J. Schwab et al., “Upper airway and soft tissue anatomy in normal subjects and patients with sleep-disordered breathing. Significance of the lateral pharyngeal walls,” Am. J. Respir. Crit. Care Med., vol. 152, no. 5 Pt 1, pp. 1673–1689, Nov. 1995.

[8] F. J. Trudo et al., "State-related changes in upper airway caliber and surrounding soft-tissue structures in normal subjects," Am. J. Respir. Crit. Care Med., vol. 158, no. 4, pp. 1259–1270, Oct. 1998.
[9] R. J. Schwab et al., "Identification of upper airway anatomic risk factors for obstructive sleep apnea with volumetric magnetic resonance imaging," Am. J. Respir. Crit. Care Med., vol. 168, no. 5, pp. 522–530, Sep. 2003.
[10] K. Nayak and R. Fleck, "Seeing Sleep: Dynamic imaging of upper airway collapse and collapsibility in children," Pulse, IEEE, vol. 5, no. 5, pp. 40–44, 2014.
[11] M. E. Wagshul et al., "Novel retrospective, respiratory-gating method enables 3D, high resolution, dynamic imaging of the upper airway during tidal breathing," Magn. Reson. Med., vol. 70, no. 6, pp. 1580–1590, Dec. 2013.
[12] R. Arens et al., "Changes in upper airway size during tidal breathing in children with obstructive sleep apnea syndrome," Am. J. Respir. Crit. Care Med., vol. 171, no. 11, pp. 1298–1304, Jun. 2005.
[13] Y.-C. Kim et al., "Measurement of upper airway compliance using dynamic MRI," in Proc. ISMRM 20th Sci. Sessions, Melbourne, Australia, 2012, vol. 20, p. 3688.
[14] Y.-C. Kim et al., "Real-timeMRI can differentiate sleep-related breathing disorders in children Introduction," in Proc. ISMRM 21st Sci. Sessions, Salt Lake City, UT, USA, 2013, vol. 21, no. c, p. 251.
[15] Y.-C. Kim et al., "Real-time 3D magnetic resonance imaging of the pharyngeal airway in sleep apnea," Magn. Reson. Med., vol. 71, no. 4, pp. 1501–1510, Apr. 2014.
[16] Y.-C. Kim et al., "Investigations of upper airway obstruction pattern in sleep apnea benefit from real-time 3D MRI," in Proc. ISMRM 22nd Sci. Sessions, Milan, Italy, 2014, no. 5, p. 4364.
[17] S. Y. Yeoa et al., "Segmentation of human upper airway using a level set based deformable model," in Proc. 13th Med. Image Underst. Anal., pp. 174–178, 2009.
[18] S. Salerno et al., "Semi-automatic volumetric segmentation of the upper airways in patients with Pierre Robin sequence," Neuroradiol. J., vol. 27, pp. 487–494, 2014.
[19] V. R. D. Water et al., "Measuring upper airway volume: Accuracy and reliability of dolphin 3D software compared to manual segmentation in craniosynostosis patients," J. Oral Maxillofac. Surg., vol. 72, no. 1, pp. 139–144, 2014.
[20] J. Liu et al., "System for upper airway segmentation and measurement with MR imaging and fuzzy connectedness,"Acad. Radiol., vol. 10, no. 1, pp. 13–24, 2003.
[21] R. Adam and L. Bischof, "Seeded region growing," IEEE Trans. Pattern Anal. Mach. Intell., vol. 16, no. 6, pp. 641–647, Jun. 1994.
[22] Daniel. (2011). Region Growing (2D/3D grayscale). [Online]. Available: http://www.mathworks.com/matlabcentral/fileexchange/32532-region-growing-2d-3d-grayscale-
[23] L. Dice, "Measures of the amount of ecologic association between species," Ecology, vol. 26, no. 3, pp. 297–302, 1945.
[24] C. W. Wang et al., "Evaluation and comparison of anatomical landmark detection methods for cephalometric X-ray images: A grand challenge," IEEE Trans. Med. Imag., 2015, to be published.
[25] P. Geurts, "Automatic Cephalometric X-Ray Landmark Detection Challenge 2014: A machine learning tree-based approach," 2014.
[26] C. Chu et al., "Fully Automatic cephalometric X-ray landmark detection using random forest regression and sparse shape composition," in Proc. ISBI International Symposium on Biomedical Imaging 2014: Automatic Cephalometric X-Ray Landmark Detection Challenge, 2014.
[27] H. Mirzaalian and G. Hamarneh, "Automatic globally-optimal pictorial structureswith random decision forest based likelihoods for cephalometric X-ray landmark detection." in Proc. ISBI International Symposium on Biomedical Imaging 2014: Automatic Cephalometric X-Ray Landmark Detection Challenge, 2014.